Applied Science Innovation (ASI)
Published by College of Physical and Applied Sciences, MOUAU

- *Received:* 20 May 2026
- *Revised*: 11 June 2026
- *Accepted:* 17 June 2026
- *Published:* 30 June 2026

CORROSION INHIBITION OF MILD STEEL IN SIMULATED MARINE ENVIRONMENT USING *FICUSSUR* LEAF EXTRACT: ELECTROCHEMICAL AND GRAVIMETRIC STUDIES

Ajike E. Emea[1*], Elizabeth C. Nwaokorongwu[2], Lebe A. Nnanna[3], Chijioke I. Oriaku[4]

[1*]Department of Physics, Clifford University, Owerrinta, Imo State, Nigeria
[234]Department of Physics, Michael Okpara University of Agriculture, Umudike, Abia State Nigeria

***Corresponding author:** emeae@cliffordуni.edu.ng, emeaajike@gmail.com

ABSTRACT

Using gravimetric and electrochemical methods, the effectiveness of Ficus sur leaf extract in preventing corrosion on mild steel in a 1 M NaCl solution was methodically assessed. Mass loss measurements showed that as inhibitor concentration increased, the corrosion rate gradually decreased. At higher temperatures, partial desorption of adsorbed species led to a drop in inhibition efficiency. At 1.0 g/L and 303 K, the highest gravimetric inhibition efficacy of almost 80% was attained. Potentiodynamic polarization (PDP) and electrochemical impedance spectroscopy (EIS) were two electrochemical tests that demonstrated markedly improved inhibitory efficiency, of 98.7% at 0.60 g/L. PDP results revealed mixed-type inhibition behavior with a significant decrease in corrosion current density (from 1819 to 23 μA cm^{-2}) and little change in corrosion potential. The creation of a protective adsorbed coating at the metal/electrolyte interface was confirmed by EIS analysis, which showed a significant increase in charge transfer resistance (up to 35,000 Ω•cm^2) and better capacitive responsiveness. Inhibitor molecule adsorption followed the Langmuir isotherm, and negative Gibbs free energy values suggested spontaneous and primarily physisorption-driven interaction. The adsorption-controlled inhibitory mechanism was further confirmed by changes in activation energy. These results demonstrate that Ficus sur extract is a safe and efficient corrosion inhibitor for mild steel in chloride-rich conditions.

Keywords: Corrosion, Inhibition, Adsorption, Isotherm, Molecule, Impedance

1. Introduction

Metal corrosion, especially that of mild steel, continues to be a significant problem in industrial systems such chemical processing equipment, pipelines, and maritime structures. Aggressive ion penetration accelerates corrosion in chloride-containing environments, such as NaCl solutions, resulting in structural deterioration and large financial losses (Verma *et al*., 2021; Zhang *et al.*, 2022). Despite their effectiveness, conventional corrosion inhibitors are frequently hazardous, costly, and harmful to the environment, which restricts their widespread use (Lgaz *et al.*, 2020). According to recent research, plant-based inhibitors with

π-electrons and heteroatoms (such O, N, and S) can adsorb onto metal surfaces to produce protective films that lower corrosion rates (Quraishi& Chauhan, 2020; Singh et al., 2022). According to a study by Emea *et al.* (2023), plant extracts decrease corrosion reactions by donating electrons to the metal's d-orbitals. *Ficus sur* leaf extract attracts more attention for research among other natural inhibitors because of its accessibility, environmental friendliness, and rich phytochemical makeup (Okafor et al., 2021).

Mild steel is still quite vulnerable to deterioration in saline settings like 1 M NaCl, despite advancements in corrosion management. Synthetic inhibitors are not widely used because of health and environmental risks. Moreover, a number of variables, including temperature, inhibitor concentration, and exposure duration, affect corrosion process (Singh et al., 2022).

Previous research have centered on plant-based corrosion inhibitors, there isn't much thorough research analysis that combines electrochemical and gravimetric methods to assess *Ficus sur* performance. Therefore, the purpose of this study is to use both gravimetric and electrochemical methods to examine how well *Ficus sur* leaf extract inhibits corrosion on mild steel in NaCl conditions.

2. Methodology

2.1. Metal preparation

Corrosion studies were performed on mild steel sheet. Prior to corrosion process, the mild steel were mechanically cut, a hole drilled at one end for free suspension and numbered by punching. The surface of each coupon were then polished using 220, 800 and 1200 emery papers to obtain a smooth area. The coupons were further degreased with acetone and rinsed with distilled water to remove debris and dried in warm air according to previous work done Khadom *et al*., (2015).

2.2. Leaf Preparation

The Leaves were dehydrated under the sun for three days. After sun drying, they were crushed to elevate the surface area and kept in a closed container. 20 grams of the crushed *Ficus sur* and (fineness: particle size of about 150-250 µm) were measured into their respective environments (200 ml of NaCl) and were heated at room temperature for 3 hours using reflux apparatus. After heating, the extracts were allowed to cool. The residues were oven dried and reweighed. Thereafter, five different concentrations of the leaves extracts which include 0.2g/L, 0.4g/L, 0.6 g/L, 0.8 g/L and 1.0 g/L were prepared (Emea *et al.*, 2023).

2.3. Gravimetric Method

In the mass loss measurements, coupons were completely immersed in 100ml of the test solution of the environments (1 M NaCl) in the presence and absence of the inhibitors (*Ficus sur* at 303K. The metal specimens were withdrawn from the test solutions after two hours interval for 10 hours. The coupons were rinsed with Nitric acid to quench the reaction, rinsed with distilled water to remove the inhibitor solution and then rinsed with ethanol and acetone to dry the coupon. The mass loss was taken as the difference in weight of the specimens before and after immersion determined using Electronic analytical balance (metlar terado) with sensitivity of 0.001g. The tests were repeated to guarantee the reliability of the results and the mean value of the mass loss eported. From the mass loss measurements, Corrosion rate was expressed in ^{mg} $_{cm\text{-}2\ hr\text{-}1}$ of the samples. The inhibition efficiency (η%) was calculated from mass loss using the following equations: (Okafor *et al.*, 2021)

$$\Delta w = (w_1 - w_2) X\, 1000 \ \ (mg) \qquad (1)$$

GALLEY PROOF

$$A = 2\left[(LXB - \frac{\pi d^2}{4}) + 2(LXH) + 2(BXH) + \pi dH\right] \quad (2)$$

$$p = \frac{w_o}{v} \quad (3)$$

$$v = (LXBXH) - \frac{\pi d^2}{4}H \quad (4)$$

$$C.R. = \frac{K\Delta w}{APT} \quad (5)$$

Where C.R.= corrosion rate, $\Delta w =$ change in weight (mg), A= cross sectional area of (cm^2) P = density of , (g/cm^3), K= 87.6 (corrosion constant), t = time of study (hrs), w_1 and w_2 are the initial and final weights of coupon. L, B, H, and d represent length, breadth, height and the diameter of the coupon. Figure 2 shows the graph of corrosion rates their respective time of exposure (room temperature) at different concentrations of the inhibitors (*Ficus sur*). Concentrations that showed better curves were selected for thermodynamic examinations.

$$\text{Inhibition efficiency \%} = \frac{W_B - W_A}{W_B} X \frac{100}{1} \quad (6)$$

Where w_B and $w_{A\ are}$ weight loss in the absence and presence of the inhibitor.

The degree of surface coverage (θ) was calculated from the weight loss measurements using Equation (7):

Surface coverage

$$\theta = \frac{W_B - W_A}{W_B} \quad (7)$$

Where w_B and w_A are the weight loss in the absence and presence of the inhibitor.

The effect of temperature on the inhibition efficiency of the inhibitor was carry out at the temperature of 303K and 318Kusing weight loss measurements.

2.4. Thermodynamic Adsorption Isotherm

2.4.1. Langmuir Isotherm

Basic information on the interaction between the inhibitor and the metal can be provided by the adsorption isotherm. The manner of adsorption (physisorption or chemisorption) is determined by the electronic structure of the metal, nature of the corrodent and the chemical nature of the inhibitor. The Langmuir adsorption isotherm equation is given by the equation 8:

$$\frac{C}{\theta} = \frac{1}{K_{ads}} + C \quad (8)$$

Where C is the concentration of *Ficusur* and θ is the surface coverage and K_{ads} is the adsorptive equilibrium constant.(Iroha and Hamilton, 2018).

The adsorption free energy (ΔG^0ads) is related to K_{ads} by the (9)

$$\Delta G^O_{ads} = -RT\ln(K_{ads} X\, 55.5) \quad (9)$$

Where R is the gas constant (8.314 kJ/mol) and T is the absolute temperature. The value 55.5 is the concentration of water in solution in mol/L. The adsorption parameters from Langmuir adsorption isotherms are estimated for 303K, 318K and 333K at different concentrations of the respective inhibitors (*Ficus sur*).

3.10.2 Thermodynamic Studies

The mode of adsorption of inhibitors which can either be physio or chemisorption may be predicted from the knowledge of thermodynamic parameters that govern the adsorption process. The activation energies

GALLEY PROOF

Ea for corrosion process in the absence and presence of leaf extract of *Ficus sur*were calculated using Arrehnius equation (10)

$$\ln W = \ln A + \frac{-E_a}{2.303RT} \quad (10)$$

Where w is the corrosion rate, A is the frequency, factor R is the gas constant and Ea is the activation energy which can be obtained when lnW is plotted against the inverse of absolute temperature 1/T. the activation energy becomes

$$E_{a= -slopeX\ 2.303XR} \quad (11)$$

Where R = 8.314 the real gas constant

2.4.2. Temkin isotherm

Equation 12 relates the degree of surface coverage (θ) and the inhibition concentration (c). After linearization using logarithmic transformation, the constant K and the parameter "a" were obtained for isotherm at various temperatures and time. From equation 12, this was achieved by making a plot of θ against logc.

$$\theta = -\frac{-2.303\ln k}{2a} - \frac{2.303\ln c}{2a} \quad (12)$$

2.5. Electrochemical Study

Electrochemical analyses were conducted in 0.5 M HCl, and 3.5% NaCl, corrosive electrolytes. To prevent charging current and confirm system stability open circuit potential (OCP) was recorded for a duration of 1800 s (30 mins). This is required for the metal to dissolves at its equilibrium or free potential (E_{corr}) which is achieved at stable OCP. Thereafter, all the electrochemical experiments were carried out at OCP condition (Singh *et al.*, 2022). The electrochemical tests were run using a cell assembly consisting of three electrodes which includes; 1 cm^2 exposed metal surface mild steel which served as the working electrodes (WE), silver/silver chloride (Ag/AgCl) was used as a reference electrode (RE); all the reported potentials in this work are vs. Ag/AgCl, while platinum wire was utilized as a counter electrode (CE). The electrochemical impedance spectroscopy (EIS) was measured with a signal amplitude perturbation of 10 mV throughout a frequency range of 100 kHz–10 mHz. The data were later analyzed using appropriate electrochemical analytical softwares such as Zsimpwin 3.2 model for EIS with the fitted equivalent circuit simulated for the specific metal/ electrolyte environment and EC-lab was utilized for the potentiodynamic polarization, analyses and all data were plotted using origin pro 2016 model software.

3. Results and Discussions

3.1. Mass loss of Mild steel in different concentrations of *Ficussur*in 1M NaCl

The rate of corrosion peaked in blank solutions and dropped as the concentration of the inhibitor increased. The effects of temperature varied according to the medium, but inhibition was always effective. The mass loss of the mild steel decreases as the inhibitor concentration rises, suggesting a charge transfer for surface covering that prevents corrosion.

GALLEY PROOF

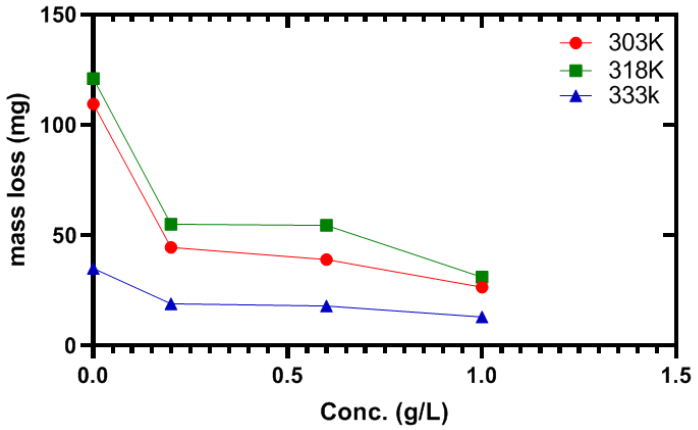


Figure 1. Mass loss of Mild steel in different concentrations of *Ficussur*in 1M NaCl at different temperatures in 2hrs.

3.2. Corrosion Rate of Mild Steel in *Ficussur* (1M NaCl)

As the concentration of the inhibitor in both media increased, the corrosion rate dropped. However, in NaCl settings, temperature had a distinct effect on corrosion, indicating medium-dependent inhibitory behavior (figure 2). The metal's surface desorption was indicated by the highest corrosion rate, which was found at 333K.

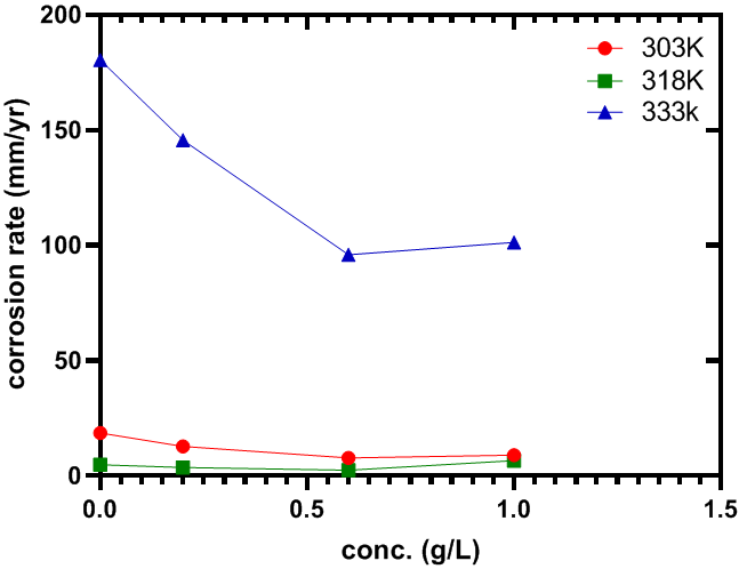


Figure 2. Corrosion rate of alloy in different concentrations of *Ficussur* in 1M NaClat different temperature in 2hours

3.3. Inhibition Efficiency of *Ficus sur* on Mild Steel in 1 M NaCl

Figure 3 illustrates that inhibitory efficiency occurred at higher doses but lower temperatures. Although overall performance remained effective, a reduction at higher temperatures suggested partial desorption of bound molecules. It was found that the highest inhibition efficiency was 80%. Furthermore, the inhibition efficacy rises with increasing inhibitor concentrations, suggesting a charge transfer and surface coverage to the mild steel. This outcome is consistent with that of Emea et al. (2023), who reported that green inhibitors prevent corrosion by transferring sigma electrons to the metal's d-orbital.

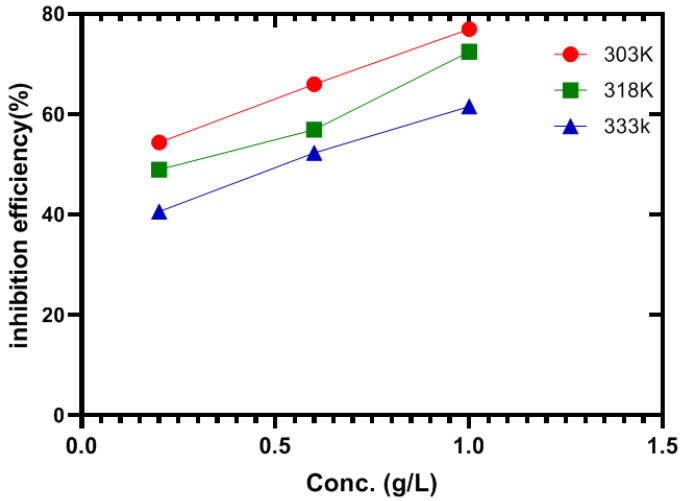


Figure 3. Inhibition efficiency of Mild steel in different concentrations of *Ficus sur* in 1M NaCl at different temperatures in 2hrs.

3.5. Thermodynamic Isotherms

3.5.1. Langmuir Adsorption Isotherm

With regression coefficients close to unity, the extract's adsorption behavior was consistent with the Langmuir isotherm. Spontaneous adsorption was suggested by negative Gibbs free energy values. As seen in Table 1 values within −20 kJ/mol indicated physisorption, which involves electrostatic charge transfer from the inhibitor molecules (heteroatoms) to the metal surfaces.

3.5.1.1. Activation Energy

Blank solutions had lower activation energy values than inhibited systems, suggesting that inhibitors reduced corrosion rates by increasing energy barriers. Negative values indicate exothermic reactions that promote metallic surface covering as shown in Table 2.

Table 1: Calculated Values Of Langmuir Isotherm Adsorption Parameter for 1 M NaCl*Ficussur*

Time (hr)	R^2	Slope	Kads	ΔGads (KJ/mol)
	303K			
2	0.8059	3.000	-8.333	-5.552
	318K			
2	0.9296	2.150	1.072	-3.696
	333K			
2	0.9907	1.413	4.181	-4.928

LEYPROOF

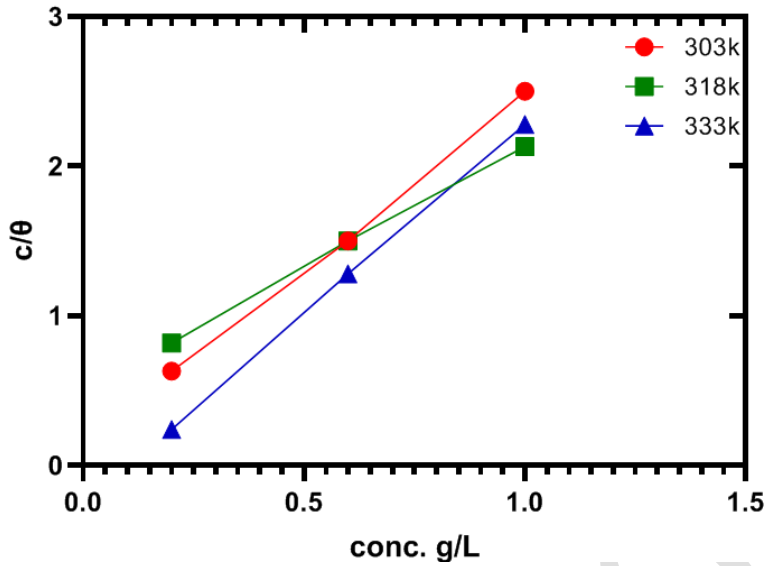


Figure 5: Langmuir isotherm of in different concentrations of *Ficussur* in 1 M NaCl in 2hrs

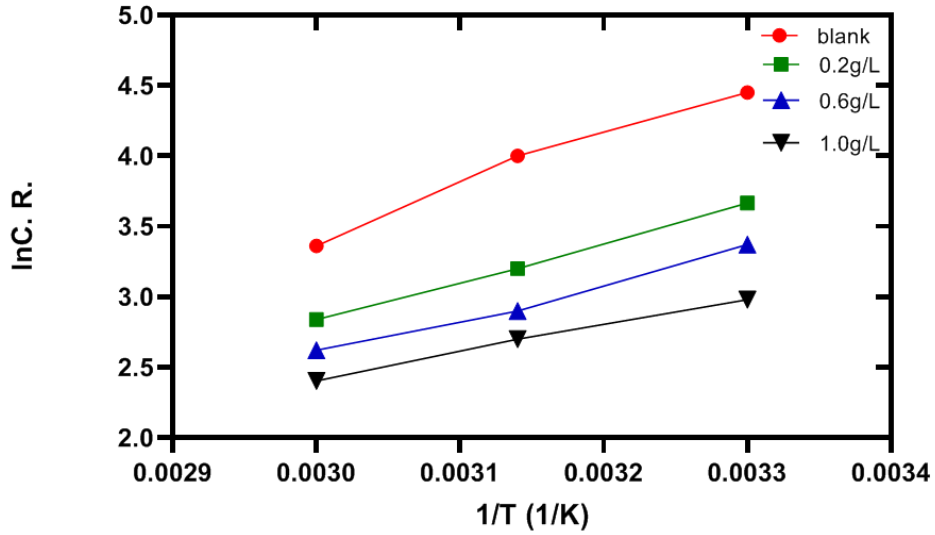


Figure 6: Plot of lnC.R. versus 1/T for Mild steel corrosion in 1.0M NaCl (Blank) and inhibited solutions at various concentrations of *Ficus sur* for 2hrs

Table 3: Activation energy value of *Ficus sur* in 1M NaCl for mild steel in 2hour

Conc. (g/L)	Slope	Activation Energy KJ/mol
Blank	3611	-691.30
0.2	2757	-527.89
0.6	2511	-480.78
1.0	1916	-366.86

3.5.2. Temkin Adsorption Isotherm

Adsorption behavior comparable with chemical adsorption was shown by Temkin isotherm plots. While Gibbs free energy estimates verified mixed physical and chemical adsorption depending on circumstances, positive interaction parameters indicated attractive forces between adsorbed molecules.

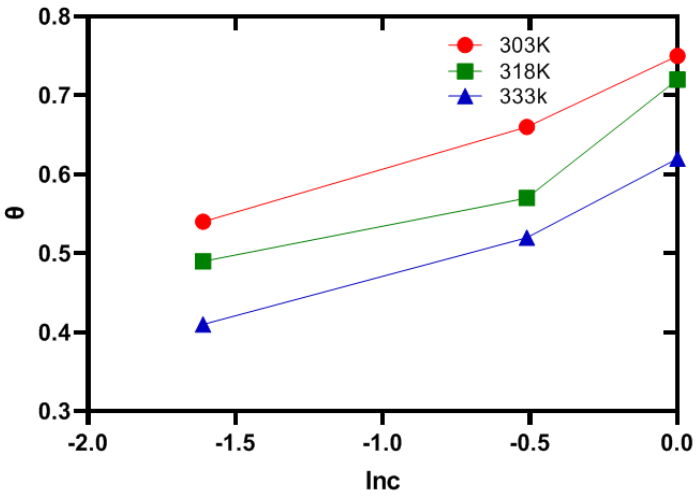


Figure 7: Temkin isotherm for adsorption of *Ficussur*on the surface of Mildsteel in 1M NaCl at 2hrs

Table 4: The parameters of Temkin parameters

Ficus sur on the surface of Mildsteel in 1M NaCl				
303	0.9843	0.1271	2.3×10^3	29.621
318	0.8612	0.1318	688.243	27.894
333	0.9678	0.1257	1.7×10^3	31.713

3.6. Open Circuit Potential (OCP) Analysis of Mild Steel in 1 M NaCl Medium at different concentrations of *Ficussur*

Figure 7 shows how the open circuit potential for mild steel changes in a 1 M NaCl solution with and without *Ficus sur* extract. The blank system has greater negative potential values which suggest that mild steel is actively corroding in the chloride-containing environment. The OCP shows a minor change toward higher positive values upon the addition of the inhibitor, indicating a decreased inclination toward corrosion. The adsorption of inhibitor molecules onto the mild steel surface, creating a barrier that prevents electrochemical processes, is suggested by the noble shift seen in Figure 7. The development of a protective coating and surface stabilization over time are further demonstrated by the comparatively steady potential profiles for the inhibited systems.

GALLEY PROOF

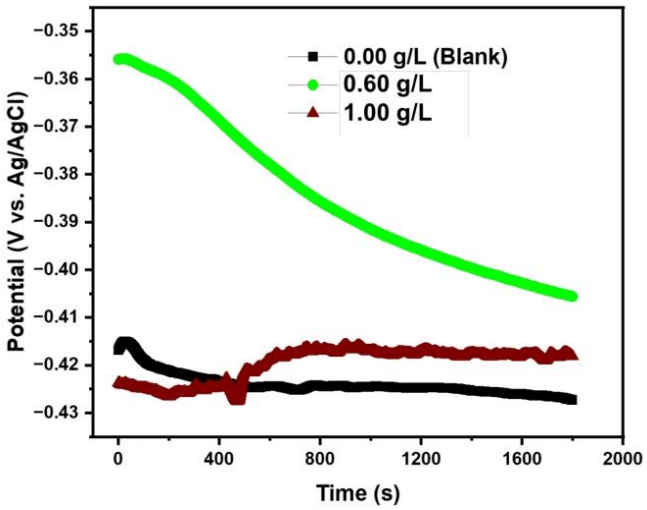


Figure 8: Open circuit potential (OCP) analysis of mild steel for blank uninhibited system in comparison with the inhibited (*Fiscus sur* extract), tested in 1 M NaCl corrosive environment at room temperature.

3.7. Potentiodynamic Polarization (PDP) Analysis of Mild Steel in 1 M NaCl Medium at different concentrations of *Ficussur*

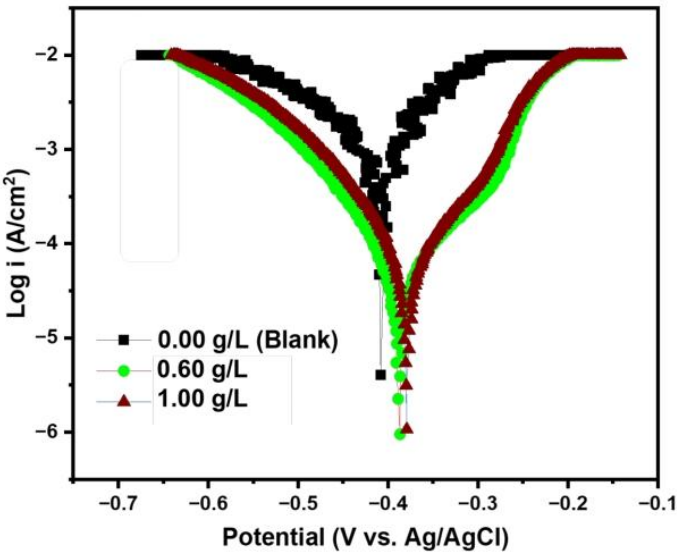


Figure 9: Potentiodynamic polarization (PDP) analysis of mild steel for blank uninhibited system in comparison with the inhibited (fiscussur extract), tested in 1 M NaCl corrosive environment at room temperature

Figure 9 displays the PDP curves for mild steel in a 1 M NaCl solution, and Table 5 summarizes the relevant electrochemical parameters. *Ficus sur* extract considerably reduces both anodic and cathodic reactions in comparison to the blank system. The corrosion current density (Icorr) values in Table 5 provide quantitative confirmation. The blank system has a high value of 1819 μA cm^{-2}, which sharply drops to 23 μA cm^{-2} at

0.60 g/L and 25 µA cm^{-2} at 1.00 g/L. This drop suggests that inhibitor adsorption has significantly reduced the rate of corrosion.

Table 5. Potentiodynamic polarization (PDP) parameters relating to mild steel for blank uninhibited system in comparison with the inhibited (fiscussur extract), tested in 1 M NaCl corrosive environment at room temperature

System	E_{corr}	I_{corr}	Ba	Bc	Θ	IE
	mV/Ag/AgCl	**µAcm^{-2}**	**mVdec^{-1}**	**mVdec^{-1}**		**%**
0.00 g/L (Blank)	-410	1819	89	120	-	-
0.60 g/L	-399	23	64	72	0.987	98.7
1.00 g/L	-398	25	71	94	0.986	98.6

Table 5's corrosion potential (Ecorr) values for the inhibited systems slightly increase from −410 mV/Ag/AgCl (blank) to about −399 mV/Ag/AgCl. This slight displacement, which is also seen in Figure 9, indicates that the inhibitor acts as a mixed-type inhibitor, affecting both cathodic oxygen reduction and anodic iron dissolution reactions (Emea *et al.*, 2023). This conclusion is further supported by the Tafel slopes (βa and βc) shown in Table 5, where the addition of the inhibitor affects both anodic and cathodic slopes. Strong adsorption and efficient surface protection are shown by the high inhibition efficiencies of 98.7% and 98.6%, as well as surface coverage (θ) values near unity.

3.8. Electrochemical Impedance Spectroscopy (EIS) Analysis of Mild Steel in NaCl Medium at different concentrations of *Ficussur*

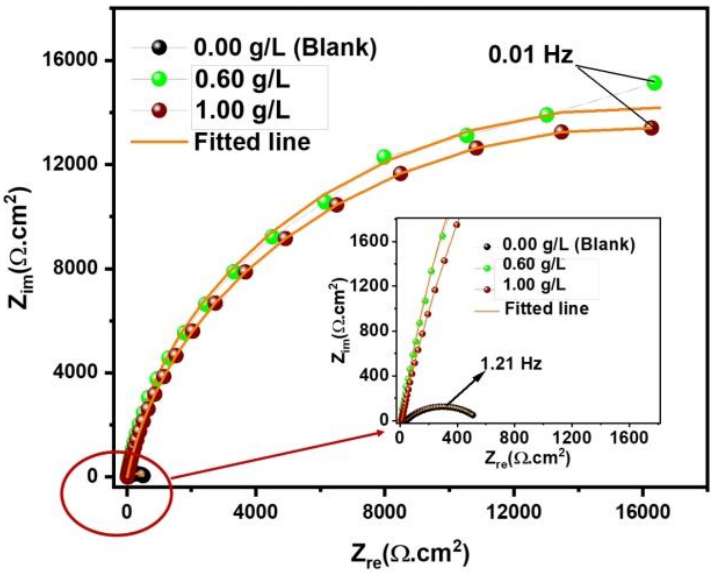


Figure 10: Nyquist plot for electrochemical impedance spectroscopy (EIS) analysis of mild steel for blank uninhibited system in comparison with the inhibited (F*icus sur* extract), tested in 1 M NaCl corrosive environment at room temperature

GALLEY PROOF

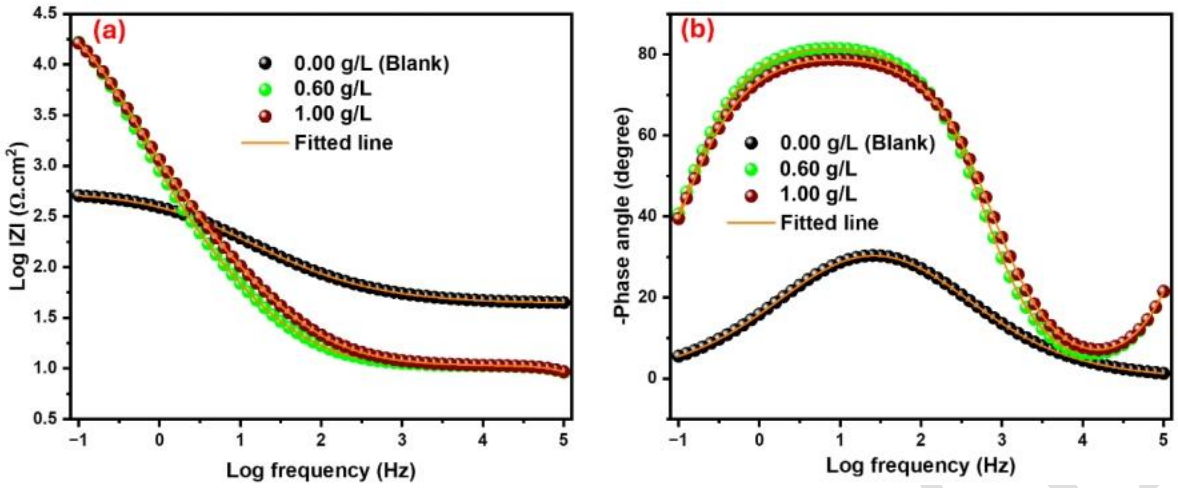


Figure 11: Bode plots (a) modulus and (b) phase angle for electrochemical impedance spectroscopy (EIS) analysis of mild steel for blank uninhibited system in comparison with the inhibited (*Ficussur* extract), tested in 1 M NaCl corrosive environment at room temperature

Figure 10 shows the Nyquist plots for mild steel in a 1 M NaCl solution with and without Ficussur extract. The uninhibited system shows a small capacitive semicircle which is a sign of significant corrosion activity and low charge transfer resistance (Rct). The semicircle's diameter greatly rises once the inhibitor is added, indicating enhanced corrosion resistance. Table 6 provides quantitative evidence for this trend, with the Rct value rising from 450 Ω•cm² for the blank to 35,000 Ω•cm² at 0.60 g/L and 31,000 Ω•cm² at 1.00 g/L. The creation of a protective coating on the mild steel surface is confirmed by the greater semicircle diameter.

Similarly, the polarization resistance (Rpo) values in **Table 6** increase markedly in the presence of the inhibitor, further indicating enhanced barrier properties and reduced corrosion rate.

Table 6: Electrochemical impedance spectroscopy (EIS) data relating to mild steel for blank uninhibited system in comparison with the inhibited (*Ficussur* extract), tested in 1 M NaCl corrosive environment at room temperature.

System	R_s (Ω. cm²)	R_{po} (Ω. cm²)	$Q1x10^{-5}$ ($\mu\Omega^{-1}s^n$ cm^{-2})	n1	R_{ct} (Ω cm²)	$Q2x10^{-5}$ ($\mu\Omega^{-1}$ $s^n cm^{-2}$)	n1	Θ	IE %
0.00 g/L (Blank)	17.91	50	87.9	0.89	450	86.77	0.89	-	-
0.60 g/L	19.07	1500	52.2	0.99	35000	55.04	0.99	0.986	98.6
1.00 g/L	18.17	1000	68.7	0.98	31000	66.29	0.98	0.984	98.4

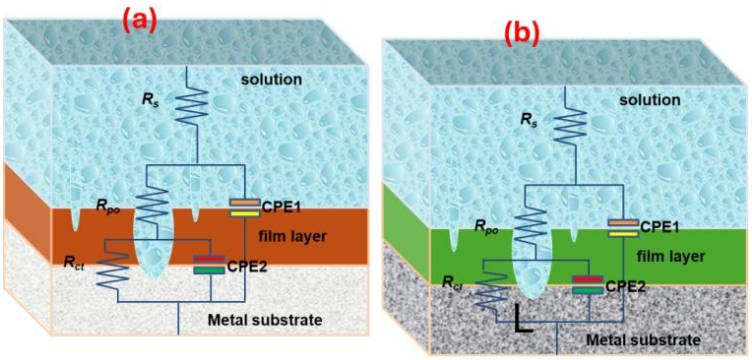


Figure 12: Electrochemical equivalenet circuit fit for blank uninhibited in comparison with the different concentrations of the inhibited tested at room temperature

Additional information about the inhibitory mechanism is provided by the Bode plots, which include the phase angle (Figure 11b) and impedance modulus (Figure 11a). The impedance modulus dramatically rises when *Ficus sur* extract is added, as seen in Figure 11a, indicating enhanced corrosion resistance. The phase angle in the inhibited systems increases toward higher values (around ed−90°) in Figure 11b, suggesting the production of a smoother and more homogenous surface as well as more perfect capacitive behavior. These findings support the idea that inhibitor molecules adsorb to form a barrier.

These results are corroborated by the constant phase element (CPE) characteristics shown in Table 6. Reduced surface heterogeneity and improved film uniformity are shown by the decrease in Q values and the increase in n values (approaching unity) in the presence of the inhibitor. These patterns are consistent with the enhanced capacitive response shown in Figure 11.

With matching surface coverage (θ) values close to unity, the inhibition efficiencies shown in Table 6 are exceptionally high, reaching 98.6% at 0.60 g/L and 98.4% at 1.00 g/L. These findings support the substantial adsorption of the inhibitor and are in line with those from PDP analysis in Table 5.

Figure 12 shows the electrochemical equivalent circuit that was utilized to match the EIS data. The circuit usually comprises of solution resistance (Rs), charge transfer resistance (Rct), polarization resistance (Rpo), and constant phase elements (CPEs) that indicate non-ideal capacitive behavior, The correctness of the suggested circuit model is confirmed by the strong agreement between the fitted and experimental data. The system's two time constants point to contributions from the adsorbed inhibitor film as well as the double layer.

4. Conclusion

In NaCl conditions, mild steel corrosion was effectively inhibited by *ficus sur* extract. Gravimetric and electrochemical tests reveal that the inhibitory mechanism includes the adsorption (physical adsorption) of phytochemicals producing a protective barrier. Furthermore, the inhibitor turned out to be a mixed sort of inhibitor.

GALLEY PROOF

References

Ajike Eziyi Emea, Lebe Agwu Nnanna, Orji Obinwa, Victor Emea Ihuoma, Elizabeth Chinyere Nwaokorongwu (2023). Investigation of the Inhibitive properties of Irvingia gabonensis extract for the corrosion of Aluminum alloy (AA4007) in 1 m HCl. Communication in Physical Sciences. 9(3):193-202*https://journalcps.com/index.php/volumes*

Iroha, N. B., & Hamilton, I. E. (2018). Adsorption and inhibitive properties of plant extract on mild steel corrosion in acidic media. *Journal of Applied Electrochemistry, 48*(10), 1121–1132. https://doi.org/10.1007/s10800-018-1234-5

Khadom, A. A., Abd, A. N., & Ahmed, N. A. (2015). Corrosion inhibition of mild steel in hydrochloric acid using plant extracts. *Journal of Materials Engineering and Performance, 24*(11), 4342–4351. https://doi.org/10.1007/s11665-015-1714-0

Lgaz, H., Salghi, R., Jodeh, S., &Hammouti, B. (2020). Green corrosion inhibitors for mild steel in acidic media: A review. *Journal of Molecular Liquids, 309*, 113102. https://doi.org/10.1016/j.molliq.2020.113102

Okafor, P. C., Ebenso, E. E., &Ekpe, U. J. (2021). Investigation of plant extracts as corrosion inhibitors for mild steel in saline environments. *South African Journal of Chemistry, 75*, 1–10. https://doi.org/10.17159/0379-4350/2021/v75a01

Quraishi, M. A., & Chauhan, D. S. (2020). Frontiers in green corrosion inhibitors for sustainable industrial processes: A review. *Materials Today Chemistry, 17*, 100297. https://doi.org/10.1016/j.mtchem.2020.100297

Singh, A., Ansari, K. R., Quraishi, M. A., &Ebenso, E. E. (2022). Mechanistic insights into corrosion inhibition of mild steel using plant-derived compounds. *Colloids and Surfaces A: Physicochemical and Engineering Aspects, 648*, 129348. https://doi.org/10.1016/j.colsurfa.2022.129348

Verma, C., Ebenso, E. E., Bahadur, I., &Quraishi, M. A. (2021). Plant extracts as green corrosion inhibitors for mild steel: Recent developments and future perspectives. *Journal of Cleaner Production, 291*, 125879. https://doi.org/10.1016/j.jclepro.2021.125879

Zhang, H., Li, X., Hou, B., & Pang, X. (2022). Adsorption and thermodynamic studies of eco-friendly corrosion inhibitors on steel in NaCl media. *Corrosion Science, 198*, 110123. https://doi.org/10.1016/j.corsci.2022.110123

GALLEY PROOF